MITSUBISHI ELECTRIC RESEARCH LABORATORIES
http://www.merl.com

BICM capacity analysis of 8QAM-alternative modulation formats in nonlinear fiber transmission

Kojima, K.; Koike-Akino, T.; Millar, D.S.; Parsons, K.

TR2015-103 September 2015

Abstract

We investigate the nonlinear performance of 8QAM-alternative 4D modulation format using GMI to evaluate the BICM capacity. Due to its constant modulus feature, the 4D-2A8PSK modulation has higher nonlinear threshold than Star- 8QAM and Circular-8QAM.

2015 Tyrrhenian International Workshop on Digital Communications

BICM capacity analysis of 8QAM-alternative modulation formats in nonlinear fiber transmission

Keisuke Kojima, Toshiaki Koike-Akino, David S. Millar, and Kieran Parsons
Mitsubishi Electric Research Laboratories
Cambridge, MA 02139-1955, USA
Telephone: +1 (617) 621–7500
Email: {kojima, koike, millar, parsons}@merl.com

***Abstract*—We investigate the nonlinear performance of 8QAM-alternative 4D modulation format using GMI to evaluate the BICM capacity. Due to its constant modulus feature, the 4D-2A8PSK modulation has higher nonlinear threshold than Star-8QAM and Circular-8QAM.**

I. Introduction

Various modulation formats have been studied for coherent optical communications [1]. 8-ary quadrature-amplitude modulation (8QAM) plays an important role in filling the gap between quaternary phase-shift keying (QPSK) and 16QAM in terms of bit rates and reach [2], [3]. It has also been proposed that 8QAM-16QAM and QPSK-8QAM are used in time-domain hybrid [4]. In order to achieve similar bit rates with improved sensitivity, subset-optimized PSK codes [5], quaternary code and sphere-cut lattice codes [6], [7], 4D honeycomb lattice codes [8], and 4-dimensional 2-ary amplitude 8-ary phase-shift keying (4D-2A8PSK) [9] have been proposed. 4D-2A8PSK is especially attractive among these 3-b/s/Hz/pol codes, since it has the properties of Gray coding and constant modulus. The latter is important for reducing the penalty due to fiber nonlinearities. Its gain over the conventional Star-8QAM is more than 1 dB in uncoded cases.

Current optical communication systems usually rely on soft-decision (SD) forward error correction (FEC) coding based on bit-interleaved coded modulation (BICM). Therefore, using the BICM mutual information, also called generalized mutual information (GMI), is a better metric for comparing multiple modulation formats. Several 8QAM constellations were compared using this metric [10] in the linear region. In this work, we extend the use of GMI to the nonlinear region for comparing two types of 8QAM, 8PSK, and 4D-2A8PSK through nonlinear fiber transmission simulations. The results show that the constant modulus property can effectively increase the margin for fiber nonlinearity.

II. Modulation Formats

In this paper, we evaluate four different modulation formats. The most common formats include the Star-8QAM and 8PSK. Circular-8QAM [11] is an improvement over Star-8QAM and 8PSK since the Euclidean distance is larger. Figure 1 shows the constellation and labeling of Star-8QAM, Circular-8QAM, and 8PSK. Constellation for the 4D-2A8PSK format [9] is shown in Fig. 2. 4D-2A8PSK and DP-8PSK are constant modulus formats, i.e., the total power summed over the two polarizations is constant at the symbol time in T-space, while the power of Star-8QAM and Circular-QAM can vary.

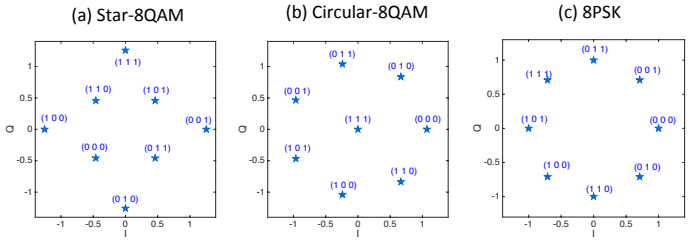

Fig. 1. Constellation and labeling [10] of (a) Star-8QAM, (b) Circular-8QAM, and (c) 8PSK.

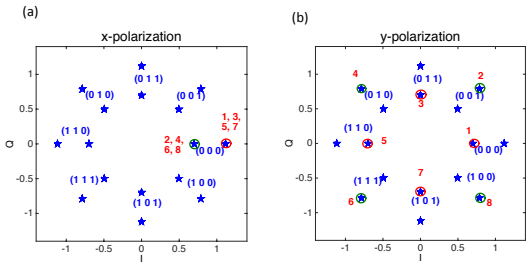

Fig. 2. Constellation and labeling of 4D-2A8PSK for (a) x-polarization, and (b) y-polarization, where (0 1 0) etc. in (a) is the first half and in (b) is the last half of the bits of the code word. Red numbers 1, 2, 3, ... represent the constellation points corresponding in x- and y-polarizations. Red and green circles in (a) and (b) indicate corresponding points in x- and y-polarizations [9]. For example, the point 2 has the code word of (0 0 0 0 0 1).

Figure 3(a) shows the dual polarization 8-ary phase-shift keying (DP-8PSK) constellation in the Stokes space, where each projected point represents 8 words of 6 bits which are actually separated well in 4D space. The nearest words in the 4D space correspond to the nearest points in Fig. 3(a). In order to increase the nearest points in the Stokes space, 4D-2A8PSK uses the constellation configuration in Fig. 3(b), where the 8 constellation points are staggered and separated into two groups. This increases the Euclidean distances.

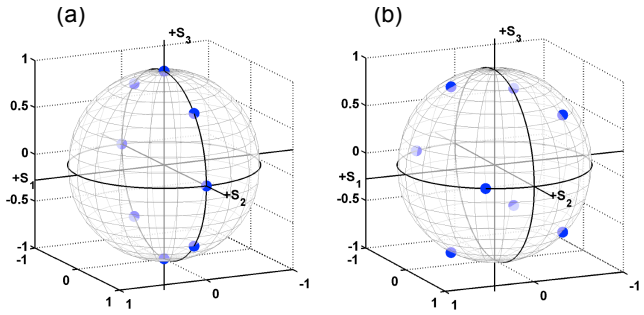

Fig. 3. Stokes representation of (a) DP-8PSK and (b) 4D-2A8PSK [9]. The nearest neighbor in 4D space corresponds to neighboring points in the Stokes space. It can be seen that the distance between points in 4D-2A8PSK is increased from that of DP-8PSK.

The 4D-2A8PSK format is expressed as

$$x(k,l) = a(k,l)\,\mathrm{e}^{\jmath\phi_k}, \quad y(k,l) = b(k,l)\,\mathrm{e}^{\jmath\phi_l},$$
$$\phi_k = \frac{\pi}{4}(k-1), \quad \phi_l = \frac{\pi}{4}(l-1),$$
$$k = 1,2,\ldots,8, \quad l = 1,2,\ldots,8,$$

where $\jmath = \sqrt{-1}$ and

$$a(k,l) = r_1, \quad b(k,l) = r_2, \quad (k+l = \text{even}),$$
$$a(k,l) = r_2, \quad b(k,l) = r_1, \quad (k+l = \text{odd}),$$
$$r_1 = \frac{\sin(\theta+\pi/2)}{\sqrt{2}}, \quad r_2 = \frac{\cos(\theta+\pi/2)}{\sqrt{2}}.$$

The ratio of the two radii r_2/r_1 determines the 4D effect. If $r_2/r_1 = 1$, the format is reduced to DP-8PSK. If $r_2/r_1 < 0.586$, 4D-2A8PSK is not Gray coded. In this paper, we use $r_2/r_1 = 0.65$, which gives the best nonlinear performance.

III. AWGN Channel Performance

We first evaluate the performance of those modulation formats in an additive white Gaussian noise (AWGN) channel. Bit error ratio (BER) was calculated as a function of signal-to-noise ratio (SNR) by Monte Carlo simulations, as shown in Fig. 4. Circular-8QAM and 4D-2A8PSK had nearly equal BER performance over the whole SNR range. Even though 8PSK is worse than other formats at high SNR regimes, it performs comparable to the other formats when SNR is low.

We then calculated GMI of the modulation formats for AWGN channels. The procedure for calculating GMI is described in [12]. Here, we chose the normalized GMI of 0.85 (GMI = 2.55 b/s/Hz/pol) as the target [10] for the state-of-the-art SD-FEC of a code rate around 0.8 [15]. Around the target code rate, Circular-8QAM is slightly better than 4D-2A8PSK, and much better than Star-8QAM and 8PSK.

IV. Optical Transmission Performance

We simulated transmission performance over a 2,000 km non-zero dispersion shifted fiber (NZDSF) link at a rate of 132 Gb/s per wavelength to investigate the effect of high fiber nonlinearity. Modulated symbols are mapped to the four

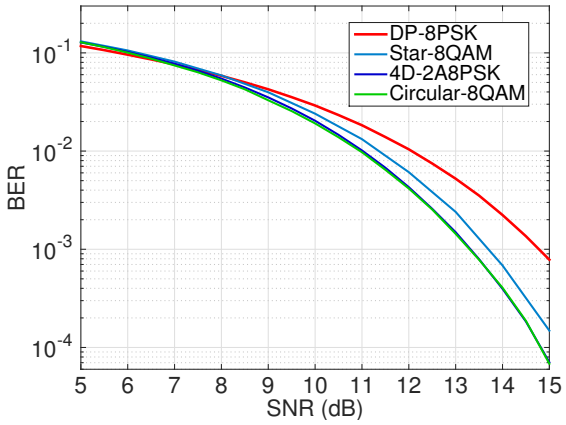

Fig. 4. BER as a function of SNR calculated for the four modulation formats.

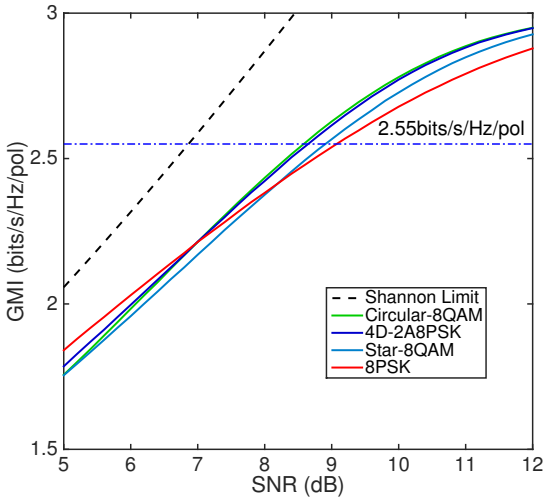

Fig. 5. GMI of the four modulation formats as a function of SNR.

dimensions (4D-2A8PSK), and two dimensions (DP-Circular-8QAM, DP-Star-8QAM, and DP-8PSK). At the transmitter, rectangular pulses were filtered by a root-raised-cosine (RRC) filter with a roll-off factor of 0.1, which drives the I/Q modulator. Five-wavelength channels with the same code were simulated with 37.5 GHz spacing and no optical filtering. The link comprises 25 spans of 80 km NZDSF with loss compensated by Erbium-doped fiber amplifiers (EDFAs). In order to quantify performance over a single link for multiple modulation formats, span loss budget was used as a performance metric [13]. NZDSF parameters were, $\gamma = 1.6$ /W/km; $D = 3.9$ ps/nm/km; $\alpha = 0.2$ dB/km. We used coupled nonlinear Schrödinger equations to model the nonlinear fiber transmission. Other fiber effects such as dispersion slope and polarization mode dispersion were not simulated. At the end of each span, 90% of the chromatic dispersion was compensated as a lumped linear dispersion compensator. No dispersion pre-compensation was introduced. An ideal homodyne coherent receiver was used, with a transfer function described by the RRC filter of a roll-off factor of 0.1, followed by sampling at twice the symbol rate. Following this, ideal chromatic dispersion equalization and data-aided least-mean-

square equalization were employed. We first used a BER threshold of 1×10^{-2} for a 20% hard decision (HD) FEC with a code rate of 0.81 [14]. All the optical noise due to the EDFA (4.0 dB noise figure) is loaded just before the receiver. The plot of span loss budget vs. launch power for the four modulation formats are given in Fig. 6.

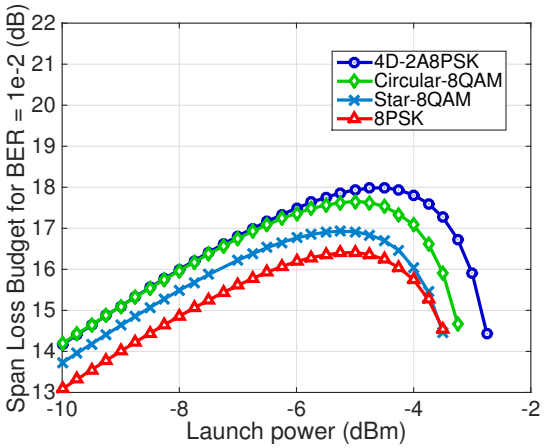

Fig. 6. Span loss budget of the four modulation formats with a target BER of 10^{-2}.

We then evaluated the span loss budget with the target GMI per bit of 0.85 (GMI $= 2.55$ b/s/Hz/pol). The optical noise is added onto the transmitted signal including nonlinear distortion, and the GMI is calculated at each optical noise level. The required optical SNR (ROSNR) is calculated such that the GMI reaches the target value. This ROSNR is used for calculating the span loss budget. The calculated span loss budget for the four formats are shown in Fig. 7. In the low launch power regime (-10 dBm) where linear propagation effects are dominant, Circular-8QAM had a slightly higher margin than 4D-2A8PSK. For higher launch powers where nonlinearity is dominant, the margin for 4D-2A8PSK becomes higher than those for Circular-8QAM and Star-8QAM by 0.27 dB and 0.98 dB, respectively, due to its constant modulus property. It is interesting to note that 8PSK gives 0.34 dB better margin than the Star-8QAM, also benefiting from the constant modulus property. In addition, Star-8QAM has larger Euclidean distance than 8PSK, yielding better BER characteristics, while 8PSK has Gray coding characteristics, giving relatively better GMI performance.

V. Conclusion

We investigated several modulation formats which has the same spectral efficiency as DP-8QAM in the presence of high fiber nonlinearity through numerical simulations, using the GMI as a metric. The recently proposed 4D-2A8PSK has 0.3 dB advantage over Circular-8QAM, and 1.0 dB over Star-8QAM. We also found that 8PSK performs better than Star-8QAM by 0.3 dB. These results indicate that constant modulus property is important to reduce the effect of fiber nonlinearity.

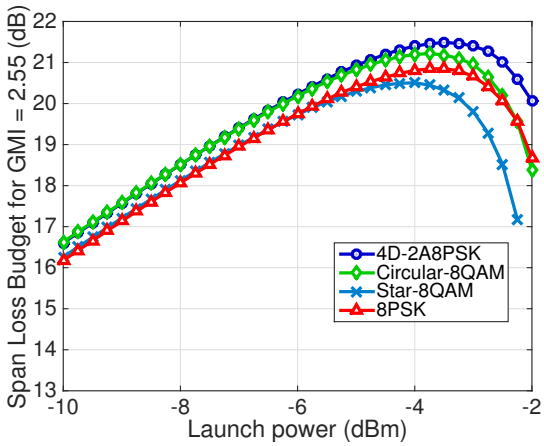

Fig. 7. Span loss budget of the 4 modulation formats with a target GMI of 2.55 b/s/Hz/pol.

References

[1] E. Agrell and M. Karlsson, "Power-efficient modulation formats in coherent transmission systems," *J. Lightw. Technol.*, vol. 27, no. 22, pp. 5115–5126, 2009.

[2] J. Zhang, H.-C. Chien, Z. Dong, Y. Xia, Y. Chen, and J. Xiao, "Transmission of 480-Gb/s dual-carrier PM-8QAM over 2550km SMF-28 using adaptive pre-equalization," *OFC*, Th4F.6, 2014.

[3] S. Zhang, F. Yaman, T. Wang, E. Mateo, T. Inoue, Y. Inada, and T. Ogata, "Transoceanic transmission of dual-carrier 400G DP-8QAM at 121.2km span length with EDFA-only," *OFC*, W1A.3, 2014.

[4] Q. Zhuge, X. Xu, M. Morsy-Osman, M. Chagnon, M. Qiu, and D. V. Plant, "Time domain hybrid QAM based rate-adaptive optical transmissions using high speed DACs," *OFC*, OTh4E6, 2013.

[5] M. Sjödin, E. Agrell, and M. Karlsson, "Subset-optimized polarization-multiplexed PSK for fiber-optic communications," *IEEE Comm. Lett.*, vol. 17, no. 5, pp. 838–840, 2013.

[6] D. S. Millar, T. Koike-Akino, S. Ö. Arik, K. Kojima, and K. Parsons, "Comparison of quaternary block-coding and sphere-cutting for high-dimensional modulation," *OFC*, M3A.4, 2014.

[7] T. Koike-Akino and V. Tarokh, "Sphere packing optimization and EXIT chart analysis for multi-dimensional QAM signaling," *ICC*, 2009.

[8] H. Buelow, X. Lu, L. Schmalen, Z. Klekamp, and F. Buchali, "Experimental performance of 4D optimized constellation alternatives for PM-8QAM and PM-16QAM," *OFC*, M2A.6, 2014.

[9] K. Kojima, D. S. Millar, T. Koike-Akino, and K. Parsons, "Constant modulus 4D optimized constellation alternative for DP-8QAM," *ECOC*, P.3.25, 2014.

[10] R. Rios-Mueller, J. Renaudier, L. Schmalen, and G. Gharlet, "Joint coding rate and modulation format optimization for 8QAM constellations using BICM mutual information," *OFC*, W3K.4, 2015.

[11] R.-J. Essiambre, G. Kramer, P. J. Winzer, G. J. Foschini, and B. Goebel, "Capacity limits of optical fiber networks," *J. Lightw. Technol.*, vol. 28, no. 4, pp. 662–701, 2010.

[12] A. Alvarado and E. Agrell, "Four-dimensional coded modulation with bit-wise decoders for future optical communications," *J. Lightw. Technol.*, vol. 33, no. 10, pp. 1993–2003, 2010.

[13] P. Poggiolini, G. Bosco, A. Carena, V. Curri, and F. Forghieri, "Performance evaluation of coherent WDM PS-QPSK (HEXA) accounting for non-linear fiber propagation effects," *Opt. Exp.*, vol. 18, no. 11, pp. 11360–11371, 2010.

[14] B. P. Smith and F. R. Kschischang, "A pragmatic coded modulation scheme for high-spectral-efficiency fiber-optic communications," *J. Lightw. Technol.*, vo. 30, no. 13, pp. 2047–2053, 2012.

[15] K. Sugihara, Y. Miyata, T. Sugihara, K. Kubo, H. Yoshida, W. Matsumoto, and T. Mizuochi, "A spatially-coupled type LDPC code with an NCG of 12 dB for optical transmission beyond 100 Gb/s," *OFC*, OM2B.4, 2013.